Hot carrier effects on the magneto-optical detection of electron spins in GaAs

T. Henn, A. Heckel, M. Beck, T. Kiessling,* W. Ossau, and L. W. Molenkamp
Physikalisches Institut (EP3), Universität Würzburg, 97074 Würzburg, Germany

D. Reuter and A. D. Wieck
Institut für Angewandte Festkörperphysik, Ruhr-Universität Bochum, 44780 Bochum, Germany
(Received 22 March 2013; revised manuscript received 29 May 2013; published 5 August 2013)

We report on spatially resolved pump-probe MOKE spectroscopy measurements of electron spins in bulk *n*-type GaAs. For low lattice temperatures these measurements are significantly compromised by local changes in the excitonic magneto-optical response which are not related to the electron spin polarization. These local changes in the excitonic Kerr spectrum are due to carrier heating caused by above-band-gap optical excitation. When hot electrons are present, a measurement of the local Kerr rotation at a fixed arbitrary probe wavelength does not necessarily correctly reveal the local electron spin polarization. By analyzing the spatial dependence of the full excitonic Kerr rotation spectrum we determine the local excitonic spin splitting energy from which we obtain the true lateral electron spin polarization profile.

DOI: 10.1103/PhysRevB.88.085303 PACS number(s): 85.75.−d, 72.25.Dc, 78.20.Ls, 75.40.Gb

Pump-probe magneto-optical Kerr (MOKE) techniques combine the advantages of high sensitivity, spatial, and temporal resolution in spin-selective spectroscopy. They have therefore been used extensively to study electron and hole spin relaxation and diffusion processes in bulk semiconductors, quantum wells, and quantum dots.[1–7]

Pump-probe MOKE spectroscopy relies on the spin selectivity of optical interband transitions in direct gap zinc-blende-type semiconductors. Electrons with a net spin polarization S_z along the z direction (sample normal) are excited by means of a circularly polarized pump laser.[8] The dynamics of the electron spin system are then probed by measuring the rotation of the major axis of polarization, the Kerr rotation θ_K, which is imposed on a linearly polarized probe laser upon reflection from the sample surface. Symmetry dictates that the Kerr rotation in polar geometry is an odd function of the local spin polarization; i.e., $\theta_K(S_z) = -\theta_K(-S_z)$ (Ref. 9). Dropping higher order contributions, a linear dependence of the Kerr rotation on the electron spin polarization $\theta_K = \alpha S_z$ is generally assumed. Systematic variation of the temporal delay Δt between short pump and probe laser pulses or the relative distance $\boldsymbol{r}$ between focused pump and probe laser beams and measurement of $\theta_K(\Delta t, \boldsymbol{r})$ is expected to reflect the time evolution and spatial dependence of the electron spin polarization $S_z(\Delta t, \boldsymbol{r})$.

In semiconductors the magnitude of the Kerr rotation depends strongly on the photon energy E_{probe} of the probe laser. The Kerr rotation is typically measured with the probe laser tuned to a wavelength near the E_0 excitonic resonance where $\theta_K(\lambda_{\text{probe}})$ is most pronounced.[5,10,11] If the magneto-optical response α in the linear relation $\theta_k = \alpha S_z$ does not depend on the coordinates $(\Delta t, \boldsymbol{r})$, MOKE spectroscopy correctly reveals the underlying spin dynamics. However, the excitonic optical resonances in semiconductors are strongly influenced by charge carrier concentration and temperature.[12–14] These parameters may significantly vary with change of the coordinates $(\Delta t, \boldsymbol{r})$, e.g., due to concurrent excess photocarrier recombination or energy relaxation of hot electrons and holes. The influence of this variation on the magneto-optical response $\alpha = \alpha(\Delta t, \boldsymbol{r})$ of the semiconductor then conceals the true spin dynamics and MOKE spectroscopy does not directly reflect the evolution of the electron spin polarization.

Here we report on spatially resolved MOKE spectroscopy measurements of electron spins in bulk *n*-type GaAs. We show that for low lattice temperatures $T_L \lesssim 25$ K these measurements are significantly altered by local changes in the excitonic resonance which are not related to the electron spin polarization. We demonstrate that the lateral Kerr rotation profile $\theta_K(r)$ does not correctly reflect the spin polarization profile $S_z(r)$ for arbitrary detection energies. We find that the local heating of the electron system caused by the above-band-gap optical excitation of the pump beam leads to a discrepancy between the Kerr rotation profile $\theta_K(r)$ and spin polarization profile $S_z(r)$. By quantitatively analyzing the full excitonic Kerr rotation spectrum $\theta_K(E_{\text{probe}})$ as a function of distance to the pump spot we recover the ability to measure the local electron spin polarization with spatially resolved MOKE spectroscopy and reveal the true lateral spin polarization profile.

The sample under investigation is a 1 μm *n*-type GaAs epilayer grown on a (001)-oriented GaAs substrate by molecular beam epitaxy. The sample structure consists of a 50 nm undoped GaAs buffer layer, a ten-period GaAs/AlAs superlattice with a period of 5 nm GaAs + 5 nm AlAs, followed by a second 50 nm undoped GaAs layer and the 1 μm Si-doped GaAs layer. The superlattice is grown to getter segregating unintentional impurities from the substrate. It also confines the photoexcited carriers to the top 1 μm GaAs layer by suppressing diffusion into the substrate. The room temperature electron density and mobility of the epilayer are $n = 1.4 \times 10^{16}$ cm^{-3} and $\mu = 5500$ cm^2 V^{-1} s^{-1} as determined by standard van der Pauw characterization. We note that our sample is very similar in both layer thickness and donor concentration to bulk GaAs samples which have been the subject of numerous previous spatially resolved Kerr and Faraday rotation spectroscopy studies.[3,5,10,11,15–18] Furthermore, we have observed results

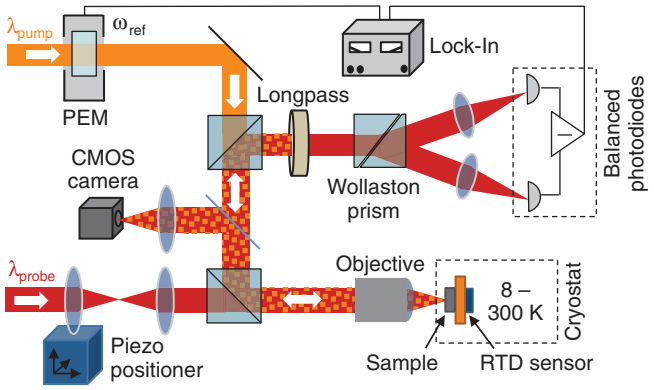

FIG. 1. (Color online) Schematic drawing of the spatially resolved two-color scanning Kerr microscopy setup.

qualitatively similar to the ones presented here in a number of samples with room temperature electron densities between 7×10^{15} cm^{-3} and 5×10^{16} cm^{-3} and layer thicknesses between 500 nm and 1 μm.

The sample is mounted strain free on the cold finger of a liquid helium flow cryostat to avoid a strain-induced splitting of the conduction band spin states which affects the electron spin dynamics.[5] The sample temperature is determined from a calibrated semiconductor resonant tunneling diode (RTD) sensor mounted to the backside of the sample holder.

Lateral profiles of the Kerr rotation $\theta_K(r)$ and spatially resolved excitonic Kerr rotation spectra $\theta_K(\lambda_{\text{probe}})$ are obtained by two-color scanning Kerr microscopy.[5,10,11] A schematic of the experimental setup is shown in Fig. 1. Localized excitation of spin-polarized electrons is provided by a continuous-wave (cw) Ti:sapphire laser (λ_{pump}), modulated between σ^+ and σ^- circular polarization at a frequency $\omega_{\text{ref}} = 50.1$ kHz by a photoelastic modulator (PEM). The photoinduced Kerr rotation θ_K of a second cw Ti:sapphire laser (λ_{probe}) is measured by a balanced photoreceiver and demodulated by a lock-in amplifier. In addition to enabling lock-in detection, modulation of the pump laser prevents unintentional polarization of the nuclear spin system by the Overhauser effect.[8] Spectral filtering of the collinear pump and probe beams is achieved by a dielectric optical longpass filter which was placed in front of the detector.

An apochromatic microscope objective ($f = 4$ mm, NA $= 0.42$) is used to focus the pump and probe laser on the sample surface. The $(1/e)$ half width of the laser spots is determined from CMOS camera images as 0.7 μm and 1.2 μm for the pump and probe beam, respectively. A net optical resolution of 1.4 μm is determined by convolution of both laser profiles. Lateral scanning of the probe spot is achieved through variation of the relative position of two aspheric lenses in confocal geometry, one of which is mounted on a piezo positioner.

All measurements are performed with the probe laser power fixed to 50 μW. The pump laser power is 10 μW and the pump wavelength is $\lambda_{\text{pump}} = 7800$ Å. Both pump and probe intensities resemble those typically found in comparable spatially resolved MOKE measurements.[5,10,11]

The setup is calibrated for quantitative measurement of the Kerr rotation θ_K. Therefore a quarter wave plate with horizontal fast axis and a PEM with peak phase retardation $\delta_r = \pi$ modulated at ω_{ref} are placed in the probe laser beam path in front of the detector. The fast axis of the PEM can be tilted by a small variable angle γ with respect to the horizontal. Variation of the PEM angle evokes a photoreceiver voltage which is demodulated at ω_{ref}. This results in a lock-in output voltage $V_{\text{LI}} \sim \gamma$. From this calibration measurement the lock-in output voltage in the MOKE experiment can be related to the absolute Kerr rotation.

The above-band-gap photoexcitation in spatially resolved MOKE spectroscopy measurements inevitably results in a local deposition of excess energy in the carrier system. It has been known for a long time that in semiconductors the electron temperature T_e can significantly exceed the lattice temperature T_L as a result of such nonresonant photoexcitation.[19–21] We have further demonstrated recently by spatially resolved photoluminescence spectroscopy that in bulk GaAs the temperature difference between the electron system and the lattice can persist over lengths exceeding ten micrometers for local excitation by a focused laser beam.[22] This effect has been observed at rather low power densities of the order of 10 W cm^{-2} for which no heating of the lattice system occurs.[22]

In spatially resolved MOKE experiments performed at low T_L we therefore expect to find a lateral gradient in the electron temperature which approaches the lattice temperature for distances far away from the pump spot. Since temperature strongly influences the excitonic optical properties of semiconductors, this lateral gradient in the electron temperature should result in a spatial variation of the local Kerr rotation spectrum $\theta_K(\lambda_{\text{probe}})$ and therefore in a position dependence of the magneto-optical response.

To demonstrate the local modification of the magneto-optical response $\alpha(r)$ by pump-induced electron heating we measure the Kerr rotation spectrum $\theta_K(\lambda_{\text{probe}})$ as a function of radial distance r between the pump and probe spot. The spectra obtained at $T_L = 8$ K at the pump spot center and in a distance of 25 μm are shown in Fig. 2(a). Both spectra are normalized to the maximum amplitude of the low-energy wing of the resonance for comparison. The Kerr spectrum exhibits an antisymmetric line shape with a zero crossing at 8189 Å (1.514 eV) which is characteristic for an energetic splitting of the $\sigma^{\pm}$ excitonic resonances.[23,24] Moving away from the pump spot we find a strong change in the Kerr spectrum in which the resonance line shape becomes significantly more narrow with increasing radial distance.

Thermal nonequilibrium between the lattice and electron system is only observed at low lattice temperatures. It results from the weak coupling between the electrons and acoustical phonons. For $T_e \gtrsim 25$ K, energy relaxation of the electron system by emission of longitudinal-optical phonons becomes efficient.[25] For lattice temperatures exceeding $\approx$25 K and cw photoexcitation, the electron and lattice system therefore are in thermal equilibrium; i.e., $T_e = T_L$.[22,26] In this case all effects due to local carrier heating vanish and the spectral shape of the excitonic Kerr resonance should be spatially homogeneous and independent of the probe laser position. In Fig. 2(b) we show that at $T_L = 30$ K the line shapes of the Kerr spectra measured at the center of excitation and at a distance of 25 μm from the pump spot indeed become identical within

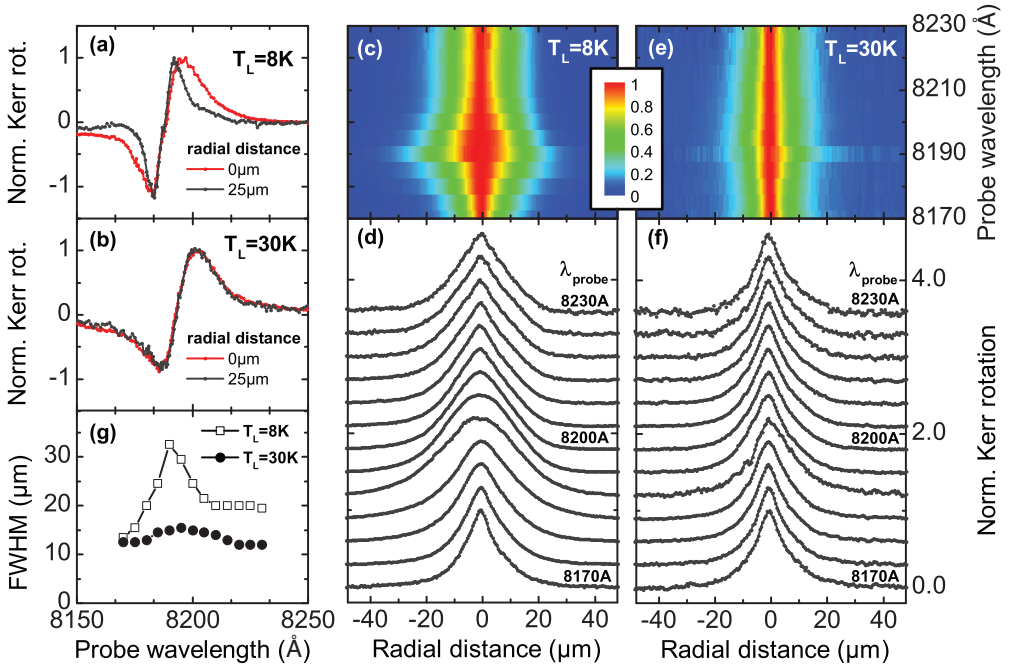

FIG. 2. (Color online) (a), (b) Normalized local Kerr spectra $\theta_K(\lambda_{\text{probe}})$ for different distances between the pump and probe spot at low (8 K) and high (30 K) lattice temperature. (c), (e) Color maps of the spatial dependence of the normalized local Kerr rotation $\theta_K(r)$ for different probe wavelengths measured between 8170 Å and 8230 Å in steps of 5 Å at low and high lattice temperature. Each $\theta_K(r)$ profile is normalized to the amplitude at the center of excitation for comparison. (d), (f) Line cuts through the same data sets. Curves are shifted vertically. (g) Full width at half maximum (FWHM) of the lateral Kerr rotation profile as a function of probe wavelength.

experimental resolution; i.e., $\theta_K(\lambda_{\text{probe}})$ does not depend on the lateral position.

We next demonstrate the consequence of the position dependence of the local magneto-optical response $\alpha(r)$ for the spatially resolved measurement of electron spin diffusion by pump-probe MOKE experiments. We have measured the lateral Kerr rotation profile $\theta_K(r)$ at $T_L = 8$ K for different probe wavelengths which were varied between 8170 Å and 8230 Å in steps of 5 Å. The λ_{probe} dependence of the profiles, normalized to the peak value at the center of the pump spot for reasons of comparison, is shown in the color map in Fig. 2(c). The individual profiles are shown as line cuts through the same data set in Fig. 2(d). Starting from short probe wavelengths, the lateral Kerr rotation profiles $\theta_K(r)$ become much wider when approaching the zero crossing of the excitonic Kerr resonance and become more narrow again when moving away from the central resonance probe wavelength [Fig. 2(c)]. Moreover, the shape of the lateral Kerr rotation profile strongly changes for probe wavelengths close to 8190 Å, as depicted in Fig. 2(d).

To quantify the above observations we plot the full width at half maximum (FWHM) of the $\theta_K(r)$ profiles as a function of λ_{probe} in Fig. 2(g). Starting from 14 μm at the shortest probe wavelength of 8170 Å, the FWHM more than doubles to values exceeding 30 μm at 8190 Å and then reduces and finally stays constant at $\approx$20 μm for long probe wavelengths $\gtrsim$8210 Å.

The decay length on which the Kerr rotation decreases to its $(1/e)$ value is closely related to the FWHM of the Kerr rotation profile. The $(1/e)$ decay length has been used in the past to extract spin diffusion coefficients in bulk n-GaAs.[10] The strong variation of the FWHM with changes in the probe wavelength observed in our measurements raises doubts on the validity of this procedure.

For $T_L = 30$ K we find that no spatial variation in the local Kerr spectrum and hence in the magneto-optical response α is present. All Kerr rotation profiles therefore are now expected to solely reflect the actual local spin polarization $S_z(r)$ irrespective of the probe wavelength. In analogy to the previous measurements we present the λ_{probe} dependence of the $\theta_K(r)$ profiles for $T_L = 30$ K in Figs. 2(e) and 2(f). In contrast to the low lattice temperature case, the width and shape of the Kerr rotation profiles now only weakly depend on λ_{probe}. The FWHM of the $\theta_K(r)$ profiles only varies between $\approx$12 μm and 15 μm as shown in Fig. 2(g).

In the following we confirm that the spatial dependence of $\theta_K(E_{\text{probe}})$ is quantitatively explained by considering thermal broadening of the excitonic resonance close to the pump spot. We first characterize the intrinsic temperature dependence of the excitonic Kerr resonance linewidth, and subsequently analyze $\theta_K(E_{\text{probe}})$ in terms of a model which relates the Kerr rotation to spin-induced modifications of the dielectric function.

The Kerr rotation θ_K of the linearly polarized probe laser results from a difference in the complex dielectric functions $\tilde{\epsilon}^{\pm}(\hbar\omega)$ for $\sigma^{\pm}$ light with photon energy $E_{\text{probe}} = \hbar\omega$. The Kerr rotation is caused by a difference in the phase jumps $\Delta^{\pm}$ of the complex amplitude reflection coefficients.[9] Starting from the explicit expression for the phase jumps under normal incidence,

$$\Delta^{\pm} = \arctan\left(-\frac{2\kappa^{\pm}}{n^{\pm 2} + \kappa^{\pm 2} - 1}\right), \qquad (1)$$

we can relate the Kerr rotation[9]

$$\theta_K = -\tfrac{1}{2}(\Delta^+ - \Delta^-) \tag{2}$$

to the respective dielectric functions via the well-known relation $\tilde{n}^\pm = (\tilde{\epsilon}^\pm)^{1/2}$ for the complex index of refraction $\tilde{n}^\pm = n^\pm - i\kappa^\pm$.

Following the concept of Ref. 24 we model the dielectric function for the energy range of interest in terms of a Lorentzian resonance representing the excitonic contribution and a static background $\epsilon_b = 11.95$ (Ref. 27) resulting from higher-energy transitions:

$$\tilde{\epsilon}^\pm(\hbar\omega) = \epsilon_b + \frac{A^\pm}{E_0^\pm - \hbar\omega + i\Gamma}. \tag{3}$$

Here, E_0^+ (E_0^-) and A^+ (A^-) are the resonance energy and amplitude for the optical transition involving σ^+ (σ^-) photons. The parameter Γ describes the linewidth of the excitonic resonance.

The influence of an imbalance of the resonance amplitudes $A^\pm$ and a splitting of the resonance energies $E_0^\pm$ on the spectral shape of the Kerr resonance is discussed in detail in Ref. 23. A difference in the resonance amplitudes $A^\pm$ results in a contribution to the spectral dependence of the Kerr rotation which is symmetric with respect to the resonance energy and does not possess a sign change. In contrast, an energetic splitting of the excitonic resonances $\Delta E = (E^+ - E^-)$ leads to a spectral dependence of the Kerr rotation on the probe laser energy which is antisymmetric and exhibits a zero crossing at the mean resonance energy as observed in our experiments.

We first examine the intrinsic electron temperature dependence of $\theta_K(E_{\text{probe}})$. We achieve experimental conditions in which the value of T_e is not influenced by optical excitation by strongly defocusing the pump and probe beams to a spot size $\gtrsim$100 μm while keeping both laser powers fixed. We thus are able to measure the Kerr spectrum for excitation densities well below 100 mW cm^{-2}. For these low excitation densities an upper bound of the excess photocarrier density is estimated to be of the order of 1×10^{14} cm^{-3}. Because of the high extrinsic electron concentration of 1.4×10^{16} cm^{-3} of the sample under investigation, pump-induced carrier heating is negligible for these low excitation densities and $T_e = T_L$ for the temperature range of interest.[28]

For the low excitation density measurements, no calibration for the detection of absolute Kerr angles is available and therefore we cannot determine the absolute value ΔE of the spin splitting. However, we are able to extract the intrinsic temperature dependence of the linewidth $\Gamma(T)$ which is independent of the absolute magnitude of the spin splitting and Kerr rotation spectrum. In Fig. 3(a) we show the normalized Kerr spectrum $\theta_K(E_{\text{probe}})$ for lattice temperatures T_L ranging from 8 K to 25 K obtained under low excitation density conditions together with the best fits derived from the Lorentzian resonance model Eqs. (1)–(3).

The intrinsic temperature dependence of the excitonic linewidth $\Gamma(T)$ obtained from these fits is shown in Fig. 3(b). The linewidth is found to monotonically increase from a low temperature value of (1.2 ± 0.1) meV at $T_L = 8$ K to (2.1 ± 0.1) meV at $T_L = 25$ K, reflecting increased thermal broadening of the excitonic resonance at

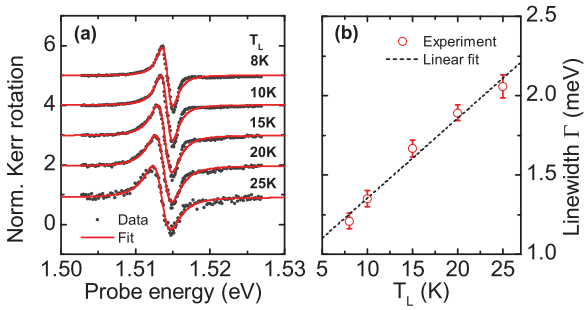

FIG. 3. (Color online) (a) Lattice temperature dependence of the normalized excitonic Kerr spectra $\theta_K(E_{\text{probe}})$ under low excitation density conditions (strongly defocused pump and probe spots). Markers are experimental data; solid lines are fits to a Lorentzian excitonic resonance model (see text). Curves are shifted vertically. (b) Temperature dependence of the linewidth $\Gamma(T_L)$ of the excitonic Kerr resonance. The dashed line is a linear fit.

higher temperatures. The broadening of the excitonic resonance results from the interaction with acoustical and optical phonons and scattering from crystal impurities and imperfections.[13,14,29] For bulk semiconductors the temperature dependence of the excitonic linewidth is of the general form

$$\Gamma(T) = \Gamma_0 + aT + bN_{\text{LO}}(T), \tag{4}$$

where the terms on the right-hand side of the equation describe the contributions of scattering with impurities, acoustical phonons, and longitudinal-optical (LO) phonons.[13] N_{LO} is the usual Bose-Einstein distribution function. For the low lattice temperatures examined in this work, scattering with LO phonons is negligible and we expect a linear dependence of the linewidth on temperature.[30] From a linear fit to the remaining part of Eq. (4) shown in Fig. 3(b) we obtain $\Gamma_0 = (0.85 \pm 0.07)$ meV and a slope $a = (0.050 \pm 4)$ meV K^{-1}. This calibration measurement allows us to deduce the local electron temperature profile $T_e(r)$.

We now turn to the analysis of the spatial dependence of the local excitonic Kerr rotation spectrum. In Fig. 4(a) we show the spectra $\theta_K(E_{\text{probe}})$ for distances of 0 μm to 25 μm to the pump spot measured in steps of 2.5 μm at $T_L = 8$ K together with the best fits derived from the Lorentzian excitonic resonance model. For the resonance amplitude $A^\pm$ of the sample under investigation we assume a value of 2.35 meV which is found in Ref. 31 for bulk GaAs of comparable impurity concentration. We note that due to the dependence of the absolute value of the Kerr rotation on both the amplitude $A^\pm$ and ΔE this introduces an uncertainty in the absolute values obtained for the spin splitting. However, since an identical value for $A^\pm$ is used for fitting all local Kerr spectra, relative changes in $\Delta E(r)$ and hence the general form of the spatial dependence of the spin splitting are not affected by this uncertainty.

To account for possible phase space filling effects due to spin-selective Pauli blockade of occupied final states,[32–34] we further allow for a reduction of the resonance amplitude A^+ for transitions involving the majority spin population as a final state in our fitting routine. We find that the relative reduction never exceeds 2% and systematically decreases when moving away from the pump spot (not shown here). This rather small reduction of the excitonic absorption is expected in

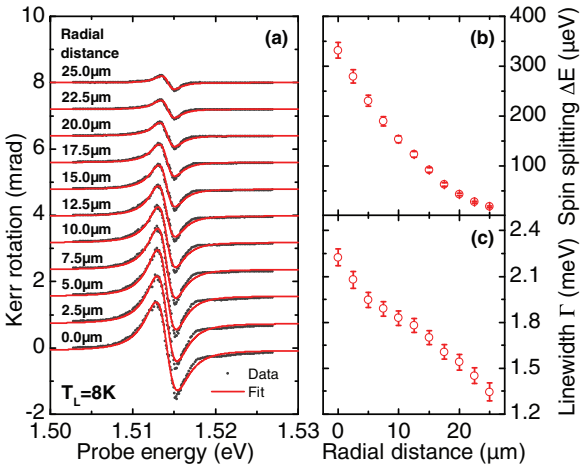

FIG. 4. (Color online) (a) Local Kerr spectrum $\theta_K(E_{\text{probe}})$ measured at increasing distances between the pump and probe spot at $T_L = 8$ K. Curves are shifted vertically. Solid lines are fits to a Lorentzian excitonic resonance model (see text). (b) Lateral profile of the excitonic spin splitting $\Delta E(r) \sim S_z(r)$ obtained from the model. (c) Local excitonic linewidth $\Gamma(r)$.

bulk semiconductors in which phase space filling is of minor importance compared to low-dimensional systems. We further note that the influence of the introduction of this additional degree of freedom to the fit on the results for ΔE and Γ is negligible.

In Figs. 4(b) and 4(c) we show the spatial dependence of the local excitonic spin splitting $\Delta E(r)$ and the excitonic linewidth $\Gamma(r)$. We find that both quantities systematically decrease with increasing distance to the pump spot, reflecting lateral electron spin diffusion and hot carrier energy relaxation, respectively.

Previously, we have reported on the local electron temperature resulting from above-band-gap photoexcitation by means of spatially resolved photoluminescence spectroscopy.[22,35] Here we employ the spatially resolved measurement of the local excitonic linewidth as a tool for the determination of the lateral electron temperature profile. In Fig. 5 we plot $T_e(r)$ which we calculated from the spatial dependence of $\Gamma(r)$

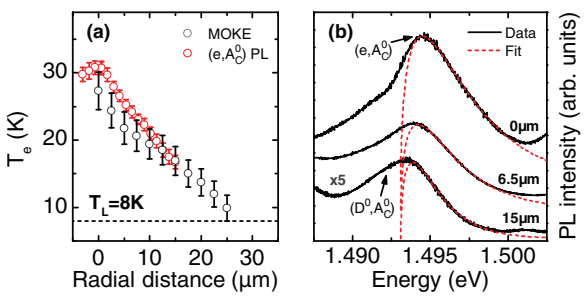

FIG. 5. (Color online) (a) Lateral electron temperature profile $T_e(r)$ obtained from spatially resolved measurements of the local excitonic resonance linewidth $\Gamma(r)$ (black circles) and spatially resolved (e,A^0_C) photoluminescence spectroscopy (red circles). The dashed horizontal line indicates the lattice temperature $T_L = 8$ K. (b) Photoluminescence spectra (black lines) obtained for a distance of 0 μm, 6.5 μm, and 15 μm to the pump spot. Red dashed lines are fits to the (e,A^0_C) transition from which T_e is deduced. Curves are shifted vertically.

shown in Fig. 4(c) and the parameters obtained from the linear fit to the low excitation density calibration measurement of $\Gamma(T)$ shown in Fig. 3(b). At the center of excitation we find a peak electron temperature $T_{e,\max} = (27.3 \pm 2.8)$ K. Moving away from the pump spot the electron temperature systematically decreases and approaches $T_L = 8$ K for distances $\gtrsim 25$ μm.

To check the validity of the determination of the $T_e(r)$ profile from the local excitonic linewidth we perform complementary spatially resolved photoluminescence measurements. In analogy to the experiments presented in Refs. 22 and 35 we determine the local electron temperature from a careful line-shape analysis of the conduction band to neutral carbon acceptor (e,A^0_C) transition.[36] Local photoexcitation at 785 nm is performed by a diode-pumped solid state laser. The pump laser is focused on the sample surface with a microscope objective (NA = 0.4, $f = 10$ mm). The luminescence light is collected by the same microscope objective and focused by a lens ($f = 250$ mm) on the entrance slit of a monochromator. The luminescence is analyzed by a 1000 mm focal length Czerny-Turner spectrometer which is equipped with a 1200 mm^{-1} grating and a CCD-array detector. The $(1/e)$ half width of the laser spot is determined from a CCD image as 1.8 μm. A pump power of 10 μW is used, resulting in excitation conditions similar to our MOKE measurements and allowing for direct comparison of results obtained from both experiments.

In Fig. 5(b) we show representative photoluminescence spectra obtained at a distance of 0 μm, 6.5 μm, and 15 μm to the pump spot. Close to the pump spot the photoluminescence spectrum in the energy range of interest is dominated by the (e,A^0_C) transition occurring at 1.4931 eV.[27] Moving away from the pump spot the (e,A^0_C) transition becomes increasingly disturbed by the nearby (D^0,A^0_C) donor acceptor pair transition at slightly lower photon energies. Together with the experimental data we show in Fig. 5(b) the best fits (red dashed lines) obtained from the (e,A^0_C) line-shape analysis from which we obtain the local electron temperature. In accordance with previous studies on the same sample[35] we find that for distances to the pump spot exceeding ≈ 15 μm the high-energy tail of the (e,A^0_C) transition becomes disturbed by the donor-acceptor pair transition. This prevents a reliable extraction of $T_e(r)$ from the (e,A^0_C) photoluminescence for larger distances.

We now compare the results for the lateral $T_e(r)$ profile obtained from our MOKE and photoluminescence measurements in Fig. 5(a). Overall we find that the spatial dependence of $T_e(r)$ obtained from the measurement of the local excitonic linewidth is well reproduced by the photoluminescence results. Minor deviations between both data sets occur very close to the pump spot where the values obtained from photoluminescence exceed T_e as determined from the MOKE experiment. These deviations can possibly be attributed to a small difference in the respective pump spot sizes which results in slightly different excitation conditions.

We finally demonstrate how spatially resolved measurements of the full excitonic Kerr spectrum can be used to correctly determine the lateral electron spin polarization profile. In the preceding section we have found that the excitonic Kerr rotation stems from an energetic spin splitting

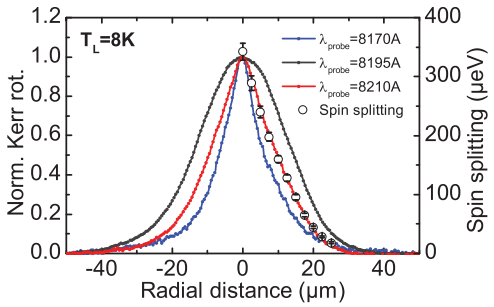

FIG. 6. (Color online) Comparison of the normalized lateral Kerr rotation profiles $\theta_K(r)$ obtained for different probe wavelengths and the lateral spin splitting profile $\Delta E(r) \sim S_z(r)$ (see text).

ΔE of the exciton resonance energies $E^{\pm}$ for $\sigma^{\pm}$ photons. Such a splitting has been observed previously in transient pump-probe transmission spectroscopy experiments[37] as well as in photoluminescence measurements in GaAs quantum wells[38–40] and recently in bulk GaAs and AlGaAs samples.[41]

From theory it is expected that this spin splitting is proportional to the density difference between spin-up and spin-down electrons; i.e., $\Delta E \sim (n_\uparrow - n_\downarrow)$.[42] Owing to the relatively high intrinsic carrier concentration of the examined sample, the pump-induced change in the total electron density $(n_\uparrow + n_\downarrow)$ is small. We therefore can directly determine the local electron spin polarization $S_z(r) = [n_\uparrow(r) - n_\downarrow(r)]/[n_\uparrow(r) + n_\downarrow(r)] \sim \Delta E(r)$ from the lateral profile of the local exciton spin splitting.

In Fig. 6 we show the lateral profile of the spin splitting $\Delta E(r)$ together with several representative normalized $\theta_K(r)$ profiles obtained at different probe wavelengths. Comparing both data sets we find a strong difference between the lateral Kerr rotation profile $\theta_K(r)$ measured at $\lambda_{\text{probe}} = 8195$ Å and the spin splitting profile $\Delta E(r) \sim S_z(r)$. We therefore conclude that the common practice[5,10,11] of probing the spin polarization with λ_{probe} tuned to the maximum amplitude of the Kerr spectrum is detrimental to a correct determination of the lateral spin polarization profile at low lattice temperatures. However, the Kerr rotation profile measured at $\lambda_{\text{probe}} = 8210$ Å perfectly coincides with the position dependence of the excitonic spin splitting $\Delta E(r)$. Comparing this result and Fig. 6 we find that the Kerr rotation profiles $\theta_K(r)$ measured with long probe wavelengths $\lambda_{\text{probe}} \gtrsim 8210$ Å, i.e., detuned from the Kerr resonance energy, indeed correctly reflect the true local electron spin polarization.

To summarize our results, we have found that at low lattice temperatures the local photoexcitation of spin-polarized electrons in bulk GaAs also results in a lateral gradient of the electron temperature. This in turn introduces a spatially varying linewidth of the local Kerr spectrum which results from local thermal broadening of the excitonic resonance. This local variation of the magneto-optical response is superimposed on the electron spin related spatial dependence of the Kerr rotation. It prevents a reliable extraction of the lateral spin polarization profile from measurements of the lateral Kerr rotation profile at a fixed, arbitrary probe wavelength.

To correctly determine the local electron spin polarization we quantitatively analyzed the full excitonic Kerr spectrum in terms of a model from which we extracted the local spin splitting. We further found that the lateral spin polarization profile is also correctly obtained from fixed-wavelength measurements of the lateral Kerr rotation profile performed at long probe wavelengths well below the excitonic resonance energy.

The authors gratefully acknowledge support by the DFG (SPP1285 OS98/9-3 and RE1507/3-3).

*tobias.kiessling@physik.uni-wuerzburg.de

[1] J. M. Kikkawa, I. P. Smorchkova, N. Samarth, and D. D. Awschalom, Science **277**, 1284 (1997).
[2] J. M. Kikkawa and D. D. Awschalom, Phys. Rev. Lett. **80**, 4313 (1998).
[3] J. M. Kikkawa and D. D. Awschalom, Nature (London) **397**, 139 (1999).
[4] Y. Ohno, R. Terauchi, T. Adachi, F. Matsukura, and H. Ohno, Phys. Rev. Lett. **83**, 4196 (1999).
[5] S. A. Crooker and D. L. Smith, Phys. Rev. Lett. **94**, 236601 (2005).
[6] J. Berezovsky, M. H. Mikkelsen, O. Gywat, N. G. Stoltz, L. A. Coldren, and D. D. Awschalom, Science **314**, 1916 (2006).
[7] T. Korn, Phys. Rep. **494**, 415 (2010).
[8] F. Meier and B. P. Zakharchenya (eds.), *Optical Orientation*, Modern Problems in Condensed Matter Sciences, Vol. 8 (North-Holland, Amsterdam, 1984).
[9] W. Reim and J. Schoenes, in *Ferromagnetic Materials. A Handbook on the Properties of Magnetically Ordered Substances*, Vol. 5, edited by K. H. J. Buschow and E. P. Wohlfahrt (North-Holland, Amsterdam, 1990), Chap. 2, pp. 133–236.
[10] M. Furis, D. L. Smith, S. Kos, E. S. Garlid, K. S. M. Reddy, C. J. Palmstrom, P. A. Crowell, and S. A. Crooker, New J. Phys. **9**, 347 (2007).
[11] J.-H. Quast, G. V. Astakhov, W. Ossau, L. W. Molenkamp, J. Heinrich, S. Höfling, and A. Forchel, Phys. Rev. B **79**, 245207 (2009).
[12] R. Leite, J. Shah, and J. Gordon, Phys. Rev. Lett. **23**, 1332 (1969).
[13] S. Rudin, T. L. Reinecke, and B. Segall, Phys. Rev. B **42**, 11218 (1990).
[14] H. Qiang, F. H. Pollak, C. M. Sotomayor Torres, W. Leitch, A. H. Kean, M. A. Stroscio, G. J. Iafrate, and K. W. Kim, Appl. Phys. Lett. **61**, 1411 (1992).
[15] S. A. Crooker, M. Furis, X. Lou, C. Adelmann, D. L. Smith, C. J. Palmstrom, and P. A. Crowell, Science **309**, 2191 (2005).
[16] M. Hruška, Š. Kos, S. A. Crooker, A. Saxena, and D. L. Smith, Phys. Rev. B **73**, 075306 (2006).
[17] M. Furis, D. L. Smith, and S. A. Crooker, Appl. Phys. Lett. **89**, 102102 (2006).
[18] S. A. Crooker, M. Furis, X. Lou, P. A. Crowell, D. L. Smith, C. Adelmann, and C. J. Palmstrom, J. Appl. Phys. **101**, 081716 (2007).

[19]J. Shah and R. Leite, Phys. Rev. Lett. **22**, 1304 (1969).
[20]R. G. Ulbrich, Phys. Rev. B **8**, 5719 (1973).
[21]R. G. Ulbrich, Solid-State Electron. **21**, 51 (1978).
[22]T. Kiessling, J.-H. Quast, A. Kreisel, T. Henn, W. Ossau, and L. W. Molenkamp, Phys. Rev. B **86**, 161201(R) (2012).
[23]A. V. Kimel, V. V. Pavlov, R. V. Pisarev, V. N. Gridnev, F. Bentivegna, and T. Rasing, Phys. Rev. B **62**, R10610 (2000).
[24]W. Maślana, W. Mac, J. A. Gaj, P. Kossacki, A. Golnik, J. Cibert, S. Tatarenko, T. Wojtowicz, G. Karczewski, and J. Kossut, Phys. Rev. B **63**, 165318 (2001).
[25]E. M. Conwell, *Solid State Physics*, edited by H. Ehrenreich, F. Seitz, and D. Turnbull, Suppl. 9 (Academic, New York, 1967).
[26]H. Münzel, A. Steckenborn, and D. Bimberg, J. Lumin. **24/25**, 569 (1981).
[27]M. R. Brozel and G. E. Stillmann (eds.), *Properties of Gallium Arsenide*, 3rd ed. (INSPEC, The Institution of Electrical Engineers, London, 1996).
[28]Negligibility of pump-induced carrier heating under defocused excitation conditions is also assured by further increasing the pump and probe spot size at fixed laser powers and comparing the normalized Kerr rotation spectra to the data presented here. It is found that a further decrease in pump intensity does not modify the linewidth of the Kerr spectrum and we thus measure the intrinsic excitonic linewidth for the given lattice temperature.
[29]V. L. Alperovich, V. M. Zaletin, A. F. Kravchenko, and A. S. Terekhov, Phys. Status Solidi B **77**, 465 (1976).
[30]D. Gammon, S. Rudin, T. L. Reinecke, D. S. Katzer, and C. S. Kyono, Phys. Rev. B **51**, 16785 (1995).
[31]S. Adachi, Phys. Rev. B **41**, 1003 (1990).
[32]S. Hunsche, K. Leo, H. Kurz, and K. Köhler, Phys. Rev. B **49**, 16565 (1994).
[33]S. Schmitt-Rink, D. S. Chemla, and D. A. B. Miller, Phys. Rev. B **32**, 6601 (1985).
[34]A. Thilagam, J. Phys. Chem. Solids **60**, 497 (1999).
[35]J.-H. Quast, T. Henn, T. Kiessling, W. Ossau, L. W. Molenkamp, D. Reuter, and A. D. Wieck, Phys. Rev. B **87**, 205203 (2013).
[36]D. M. Eagles, J. Phys. Chem. Solids **16**, 76 (1960).
[37]J. B. Stark, W. H. Knox, and D. S. Chemla, Phys. Rev. B **46**, 7919 (1992).
[38]T. Amand, X. Marie, B. Baylac, B. Dareys, J. Barrau, M. Brousseau, R. Planel, and D. J. Dunstan, Phys. Lett. A **193**, 105 (1994).
[39]L. Viña, L. Muñoz, E. Pérez, J. Fernández-Rossier, C. Tejedor, and K. Ploog, Phys. Rev. B **54**, R8317 (1996).
[40]G. Aichmayr, L. Viña, S. P. Kennedy, R. T. Phillips, and E. E. Mendez, Phys. Status Solidi A **190**, 615 (2002).
[41]E. V. Kozhemyakina, K. S. Zhuravlev, A. Amo, D. Ballarini, and L. Viña, Appl. Phys. Lett. **95**, 182107 (2009).
[42]J. Fernández-Rossier, C. Tejedor, L. Muñoz, and L. Viña, Phys. Rev. B **54**, 11582 (1996).